THE EFFECT OF TEMPERING TEMPERATURE ON THE HIGH CYCLE FATIGUE PROPERTIES OF HIGH STRENGTH SPRING STEELS

K. A. LEE, *W. J. NAM, *S. J. YOO, N. J. KIM and C. S. LEE
Center for Advanced Aerospace Materials,
Pohang University of Science and Technology, Pohang 790-784, Korea
*Steel products & welding research team, Technical research laboratories,
Pohang Iron & Steel Co., Ltd., Pohang 790-785, Korea

ABSTRACT

The high cycle fatigue behavior of a high strength spring steel has been investigated in relation to the microstructural variation through austenizing followed by tempering at different temperatures. The results have been compared with those of SAE9254 alloy which is widely used as an suspension coil spring material.

The crack initiation resistance and crack growth resistance of high strength steel, regardless of the microstructure (tempering temperature), were superior to those of SAE9254. The highest fatigue limit, ductility and toughness were achieved by tempering the alloy at 450°C which resulted in a microstructure composed of predominately the tempered martensite with a favorable precipitation distribution. At lower tempering temperatures the existence of retained austenite induced inhomogeneous slip while at higher tempering temperatures the excessive precipitation softened the martensitic matrix. These both lead to a loss in ductility and fatigue strength.

KEYWORDS

Spring steel, Rotary-bending fatigue, Fatigue crack propagation, VC, Cementite

INTRODUCTION

Weight reduction to reduce fuel consumption is an important issue in the automotive industry. One of the best methods to achieve a significant weight reduction is to improve the design strength of suspension coil springs, and as a result, various efforts have been made to develop high strength spring steels with good sag resistance and fatigue-resistant properties. This has been done through effective heat-treatments and/or micro-alloying (Kawakami et al., 1982; Iikubo and Ito, 1986), and mechanical treatments like shot peening (Larsson et al., 1991). In an effort to improve the performance of spring steels, Pohang Iron and Steel Company (POSCO) and the Research Institute for Industrial Science and Technology (RIST) jointly developed a new alloy with very high tensile strength, good sag resistance and optimum decarburization properties. However, no information so far has been obtained with respect to the fracture and fatigue properties of this alloy.

Although several micromechanical modelings and related studies have been performed (Gustavsson and Melander, 1992 ; Larsson et al., 1993 ; Melander and Larsson, 1993) in recent years, there are insufficient data for a detailed correlation between the microstructural variables and the fatigue properties of spring steels. The present investigation has been performed to probe the fracture and fatigue behavior with respect to microstructural evolution during heat-treatment, and to compare these properties with those of SAE9254 alloy.

EXPERIMENTAL PROCEDURES

The composition of high strength steel (HSS) and SAE9254 alloy used in this study is shown in Table 1. The HSS specimens were austenized at 900 °C for 40 minutes and quenched into oil (50 ~ 60 °C). They were then tempered for 30 minutes at temperatures of 300°C, 350°C, 400°C, 450°C and 500°C, respectively, and cooled in air. The SAE9254 samples were austenized at 900°C for 40 minutes and tempered for 30 minutes at 450°C.

Table 1. Chemical composition of high strength steel (HSS) and SAE9254

	C	Si	Mn	Cr	Ni	V	Fe
HSS	0.59	2.49	0.50	0.54	1.98	0.18	Bal.
SAE9254	0.53	1.52	0.74	0.81	-	0.04	Bal.

The tensile specimens had a diameter of 4 mm and a gauge length of 30 mm. The region of gauge length was ground after heat-treating, and polished with #1500 abrasive paper. Tensile tests were conducted using an Instron 8501 machine at a cross-head speed of 5mm/min.. The ASTM CT (ASTM E399, 1988) specimens were employed for fatigue crack propagation tests, as shown in Fig. 1.

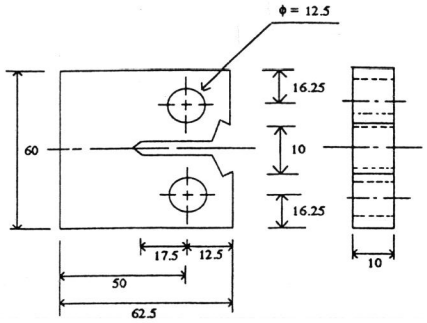

Fig. 1. Specimen configuration for fatigue crack propagation tests.

Before undertaking an actual test, 2~3 mm long precracks were made at a growth rate of 10^{-10}~10^{-9} m/cycle. The crack propagation tests were conducted under load control with sinusoidal waveform at a frequency of 10 Hz and a stress ratio of 0.1. A traveling microscope was used to monitor the advance of the fatigue crack. The crack closure load was measured by a compliance curve method. Smooth round bar specimens having a gauge length of 15.4 mm with a diameter of 8 mm were used in the rotating bending tests for the fatigue endurance

evaluation. These specimens underwent the same polishing after the heat-treatment. The endurance tests were performed in an ONO-type rotating-bending fatigue testing machine at a rate of 3500 rpm. Five specimens were used for each stress level.

The microstructures were observed by both optical microscopy and scanning electron microscopy (SEM). For a detailed understanding of the precipitates, transmission electron microscope (TEM) along with EDX was used to analyze the replicas (Cu grid).

RESULTS AND DISCUSSION

1. Characterization of microstructure

Fig. 2 shows the SEM photographs of the HSS specimens tempered at different temperatures. It is evident that all the microstructures reveal the tempered martensite structure along with the retained austenite (dark region).

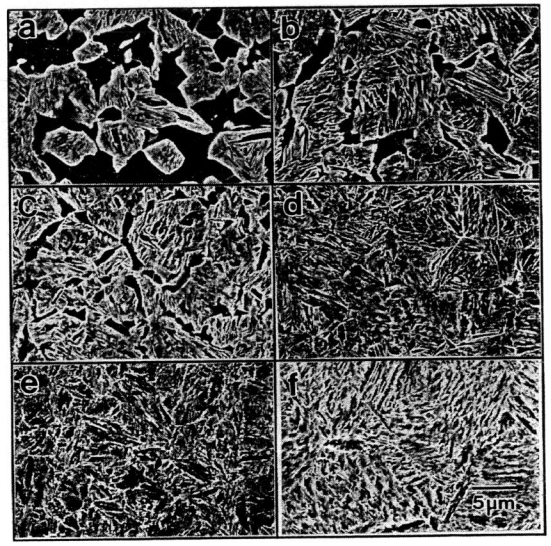

Fig. 2. SEM photographs showing microstructures tempered at
(a) 300°C (HSS) (b) 350°C (HSS)
(c) 400°C (HSS) (d) 450°C (HSS)
(e) 500°C (HSS) (f) 450°C (SAE9254).

However, with increasing tempering temperature, the amount of retained austenite progressively decreases and disappears at 450°C. As for the tempered martensite, its lath morphology is kept up to the tempering temperature of 450°C, but is modified at 500°C (Fig. 2-e).

Fig. 3 shows TEM micrographs taken from the replicas for the HSS specimens tempered at different temperatures. At 300°C, round VC(vanadium carbide) precipitates are observed to form and are distributed randomly (Fig. 3-a). Upon 350°C tempering, the size and distribution of VC are the same as those of 300°C, but its amount is larger (Fig. 3-b). Also, the spherical

cementite particles appear with a sphere at this temperature. In the case of 400°C tempering, there is no significant change in VC or the cementite. However, another type of the cementite with a needle shape appears at 400 °C. When tempered at 450°C, the precipitation of VC and cementite is basically the same as at lower temperatures, but more needle shaped cementites are found both within the lath martensite and along the lath boundary (Fig. 3-c). Finally, at 500°C tempering, the amount of precipitates increases substantially as compared to those of lower tempering temperatures. Most of the precipitates are cementites and they are found to develop not only along the lath boundary and within the lath, but also along the prior austenite boundary (Fig. 3-d).

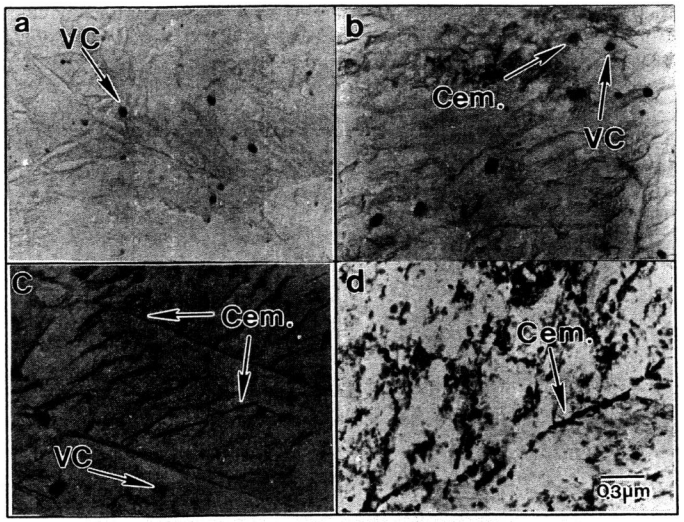

Fig. 3. TEM photographs showing various morphology of precipitates for the high strength steel tempered at (a) 300°C, (b) 350 °C, (c) 450°C and (d) 500°C.

2. Fatigue properties

In Fig. 4, the stress-life (S-N) relations are shown for the high strength steel (HSS) and SAE9254 from the rotating-bending fatigue experiments. Each data point in Fig. 4 represents an average of the values obtained from five specimens. It is noticeable that the fatigue limit of HSS, regardless of the microstructure (by tempering temperature), is higher than that of SAE9254. In the case of the HSS, the fatigue limit increases with the tempering temperature in the range of 300°C~450°C and then, starts to decrease when tempered at 500°C. The optimum condition for the fatigue endurance property is obtained at 450°C tempering temperature. Fractographic examination by SEM shows little direct evidence of crack initiation by inclusions, suggesting that this initiation mechanism is not as dominant as in other spring steels (Larsson et al., 1993; Melander and Larsson, 1993).

The fatigue crack propagation results are plotted in Fig. 5. It is found that the fatigue crack propagation properties of HSS and SAE9254 steel are almost identical. There is little change in the slopes for the HSS tempered in the range of 300°C~450°C. However, the slope of the 500°C tempered specimen is the largest though the crack growth resistance in the regime of

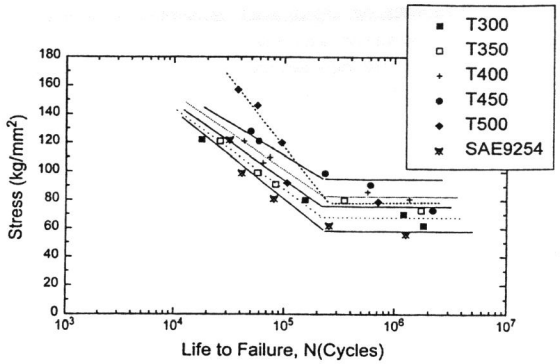

Fig. 4. S-N curves obtained by the rotating-bending fatigue tests.

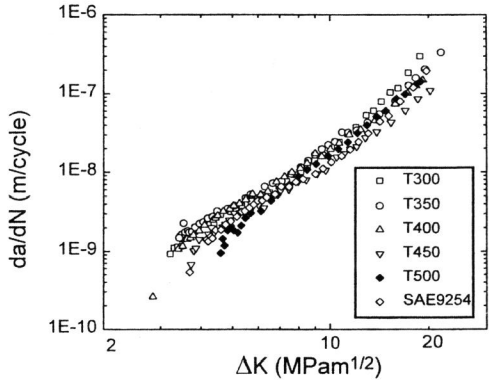

Fig. 5. Fatigue crack propagation rate (da/dN) as a function of the stress intensity factor range (ΔK).

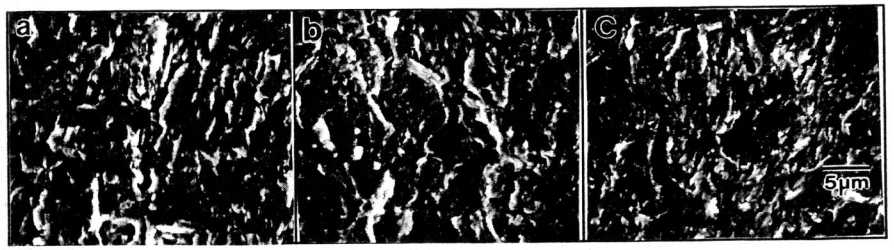

Fig. 6. SEM fractographs showing the crack propagation features for the HS spring steel tempered at (a) 300°C, (b) 400°C and (c) 500°C.

low ΔK is excellent.

Fig. 6 shows the fatigue fracture surface morphology of the specimens tempered at 300°C, 400°C and 500°C, respectively. All the specimens reveal a basically identical fatigue fracture surface, containing quasi-cleavage facets characteristic of those frequently found for the tempered martensite microstructure. The striation pattern is not evident for all the tempering conditions. The examination of crack-opening load has revealed that the crack closure effect is not sizable for the present case. This type of transgranular brittle fatigued surface correlates with the insignificant contribution of crack closure.

In response to microstructural evolution as a result of tempering, the main contributors to mechanical behavior include the retained austenite and its transformation, and the precipitation which yields different types of precipitates with various combinations of size, shape and distribution/orientation. Fig. 7 summarizes fundamental tensile properties as a function of tempering temperature for the high strength spring steel (HSS) and SAE9254 steel.

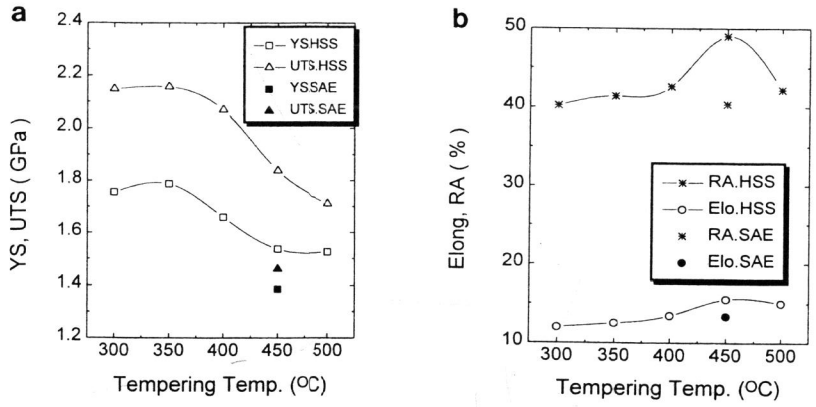

Fig. 7. Variation of (a) strength and (b) ductility for the HSS and SAE9254.

Upon tempering as low as 300°C, the steel contains appreciable amount of retained austenite (Fig. 2-a) while there exists only a primary precipitation of VC (Fig. 3-a), so both the yield strength and the ultimate tensile strength cannot attain their maximum values. For 350 °C tempering, the amount of VC precipitates is at a maximum and the V-Cr-containing cementite precipitates appear (Fig. 3-b), then the steel gets the highest strength (Fig. 7-a). As tempering temperature increases further, the strength of the steel decreases because the softening due to the tempering of martensite exceeds the strengthening due to the transformation of the retained austenite. Understandably, the tensile ductility should vary in a manner opposite to that of the strength, but there is a drop in the values of both the elongation and the reduction of area at 500 °C tempering (Fig. 7-b). This is most probably attributed to the grain boundary weakening due to intensive precipitation along the boundary, which will result in intergranular failure on considerable parts of the fracture surface.

For the present investigation, the fatigue limit varies with tempering temperature in the same manner as the ductility (Fig. 7-b). At low tempering temperatures of 300~400 °C, although the type of precipitation changes from VC to VC+$Fe_3(C,Cr,V)$, the total amount of precipitates is comparatively small and they are mostly of spherical shape. The decrease in the amount of retained austenite is assumed to be mainly responsible for the increase in fatigue

limit as tempering temperature increases. This might be attributed not only to a favorable contribution of martensite structure itself, as documented previously (Brine and Wene, 1979; Aran and Turder, 1990), but more importantly, to the slip homogeneity more realistic in a primarily single matrix microstructure (i.e. tempered martensite) than otherwise (i.e. retained austenite + tempered martensite). For the specimen tempered at 450°C, both types of precipitates, VC and $Fe_3(C,Cr,V)$, exist but their total amount is not so large as to evidently soften or decompose the martensitic matrix, which still maintains the lath characteristics (Figs. 3-c and 2-d). Moreover, the needle-shaped cementites distributed within the tempered martensite could act as obstacles to dislocation slip and thus tend to refine the slip band configuration through refining the sub-structure of the matrix (Starke and Lutjering, 1979). As a result, the material with this tempering has the maximum fatigue limit values (Fig. 4). Upon tempering at 500°C, a large amount of precipitation (Fig. 3-d) not only weakens the grain boundary, but also softens the matrix, especially the near-boundary area, causing inhomogeneous slip or slip localization. Then the fatigue limit of the steel drops (Fig. 4).

The insensitivity of the crack propagation slope to the present heat treatments (Fig. 5) is an indication that the corresponding microstructure variation does not significantly affect the dynamics of the stage II propagation behavior. Only when the precipitation is completed to such an extent as to evidently soften the tempered martensite, as occur with tempering at 500°C, does the propagation dynamics get accelerated. Nevertheless, this change is not evidenced fractographically since all the specimens exhibit a microscopically identical fatigue fracture surface (Fig. 6).

CONCLUSION

The high cycle fatigue properties of the high strength spring steel austenized at 900°C for 40 min. and tempered at the range of 300°C~500°C for 30 min. have been found to be superior to those of SAE9254 steel heat-treated in a similar manner. Due to the existence of retained austenite, the high strength steel tempered at lower temperatures (300~400°C) exhibits low values of ductility and fatigue limit. These properties also get lowered in the case of a higher tempering temperature (500°C) in which the matrix is softened considerably due to excessive precipitation. The optimum thermal treatment for obtaining good combinations of strength, ductility and fatigue resistance is to austenize the alloy at 900°C for 40 minutes and to temper at 450°C for 30 minutes. This heat treatment results in the maintenance of tempered lath martensite and the appropriate distribution of precipitations.

REFERENCES

Aran, A. and H. Turker (1990). The effect of martensite content on the fatigue behavior of a ferritic-martensitic steel. *J. Mater. Sci. Letters*, 9, 1407-1408.

ASTM E399 (1988). Metals Test Methods and Analytical Procedures. In: *Annual Book of ASTM Standards* (R. A. Storer et al. ed.), Vol. 3.01, E399-83, pp. 480-504. American Society for Testing and Materials, Philadelphia.

Brine, D. H. and E. M. Wene (1979). Fatigue in machines and structures-ground vehicles. In: *Fatigue and Microstructure*, pp. 57-99. ASM, Metals Park, Ohio.

Gustavsson, A. I. and A. Melander (1992). Fatigue limit model for hardened steels. *Fat. Fract. Eng. Mater. Struct.*, 15, 881-894.

Iikubo, T. and Y. Ito (1986). Effects of chemical composition on the strength of spring steel. *Electrical Steel-Making [in Japanese]*, 57, 33-44.

Kawakami, H., Y. Yamada, S. Ashida and K. Shiwaku (1982). SAE Technical Paper Series

820128. *SAE Transactions*, 91, 464.
Larsson, M., A. Malander, R, Blom and S. Preston (1991). Effects of shot peening on bending fatigue strength of spring steel SS 2090. *Mater. Sci. Tech.*, 7, 998-1004.
Larsson, M., A. Melander, A. Nordgren (1993). Effects of inclusions on fatigue behavior of hardened spring steel. *Mater. Sci. Tech.*, 9, 235-245.
Melander, A. and M. Larsson (1993). The effects of stress amplitude on the cause of fatigue crack initiation in a spring steel. *Int. J. Fatigue*, 2, 119-131.
Starke, Jr. E. A., and G. Lutjering (1979). Cyclic plastic deformation and microstructure. In: *Fatigue and Microstructure*, pp. 205-243. ASM, Metals Park, Ohio.

ACKNOWLEDGMENT

The authors wish to acknowledge the financial support of the Pohang Iron and Steel Company (POSCO).